Characterization of the mitochondrial genomes of two toads, *Anaxyrus americanus* (Anura: Bufonidae) and *Bufotes pewzowi* (Anura: Bufonidae), with phylogenetic and selection pressure analyses

Yu-Ting Cai[1], Qin Li[1], Jia-Yong Zhang[2], Kenneth B. Storey[3] and Dan-Na Yu[2]

[1] College of Chemistry and Life Science, Zhejiang Normal University, Jinhua, Zhejiang Province, China
[2] Key Lab of Wildlife Biotechnology, Conservation and Utilization of Zhejiang Province, Zhejiang Normal University, Jinhua, Zhejiang, China
[3] Department of Biology, Carleton University, Ottawa, Ontario, Canada

ABSTRACT

Mitogenomes are useful in analyzing phylogenetic relationships and also appear to influence energy metabolism, thermoregulation and osmoregulation. Much evidence has accumulated for positive selection acting on mitochondrial genes associated with environmental adaptation. Hence, the mitogenome is a likely target for environmental selection. The family Bufonidae (true toads) has only nine complete and four partial mitogenomes published compared to the 610 known species of this family. More mitogenomes are needed in order to obtain a clearer understanding of the phylogenetic relationships within Bufonidae that are currently controversial. To date, no mitogenomes have been reported from the genera *Anaxyrus* and *Bufotes*. *Anaxyrus americanus* can live in low temperature environments and *Bufotes pewzowi* can live in high salinity environments. We sequenced the mitogenomes of these two species to discuss the phylogenetic relationships within Bufonidae and the selection pressures experienced by specimens living in low temperature or saline environments. Like other toads, the circular mitogenomes of both species contained the typical 37 genes. *Anaxyrus americanus* had the highest A+T content of the complete mitogenome among the Bufonidae. In addition, *A. americanus* showed a negative AT-skew in the control region, whereas *Bufotes pewzowi* showed a positive AT-skew. Additionally, both toad species had unique molecular features in common: an *ND1* gene that uses TTG as the start codon, an extra unpaired adenine (A) in the anticodon arm of *trnS* (AGY), and the loss of the DHU loop in *trnC*. The monophyly of Bufonidae was corroborated by both BI and ML trees. An analysis of selective pressure based on the 13 protein coding genes was conducted using the EasyCodeML program. In the branch model analysis, we found two branches of *A. americanus* and *Bufotes pewzowi* that were under negative selection. Additionally, we found two positively selected sites (at positions 115 and 119, BEB value > 0.90) in the ND6 protein in the site model analysis. The residue D (119) was located only in *A. americanus* and may be related to adaptive evolution in low temperature environments. However, there was no evidence of a positively selected site in *Bufotes pewzowi* in this study.

INTRODUCTION

Bufonidae, the true toads, consists of 33 genera and 610 species (according to the Amphibian Species of the World 6.0, an online reference (https://amphibiansoftheworld.amnh.org/); 16 Apr. 2019) (*Frost, 2014*) and is one of the most species-rich amphibian families (*Frost et al., 2006*; *Pramuk, 2006*). However, there are only nine complete mitochondrial genomes (mitogenomes) of Bufonidae species published in GenBank along with four partial genomes (*Cao et al., 2006*; *Dong & Yang, 2016*; *Igawa et al., 2008*; *Jacob Machado et al., 2018*; *Machado, Lyra & Grant, 2016*; *Jiang et al., 2017b*; *Wang et al., 2013*; *Yang et al., 2016*; *Zhang et al., 2005*; *Zhang et al., 2013*; *Zhang et al., 2016*). These molecular data are not sufficient to represent the biodiversity of Bufonidae species. *Pauly, Hillis & Cannatella (2004)*, *Frost et al. (2006)* and *Van Bocxlaer et al. (2009)* corroborated the monophyly of Bufonidae by using partial mitochondrial DNA sequences. *Portik & Papenfuss (2015)* also confirmed the monophyly of Bufonidae, based on 243 taxa and 13 loci including nine nuclear genes and four mitochondrial genes. Furthermore, the phylogenetic relationships within Bufonidae remain controversial (*Graybeal, 1997*). As for intergeneric relationships, the genus *Bufo* was strongly confirmed as monophyletic (*Graybeal, 1997*; *Dong & Yang, 2016*). On the contrary, the polyphyly of *Bufo* was recovered in several other studies (*Maxson, 1984*; *Pyron & Wiens, 2011*; *Brandvain et al., 2014*; *Jiang et al., 2018*) and the paraphyly of South American toads was also supported (*Frost et al., 2006*; *Pramuk, 2006*).

Mitogenomes of Anura are closed, double-stranded circular molecules of about 16-24 kb in length that include 2 ribosomal RNA genes (12S and 16S rRNA), 22 transfer RNA genes (tRNAs), 13 protein-coding genes (PCGs), and one control region (CR; also known as the D-loop region) (*Kakehashi et al., 2013*; *Cai et al., 2019*). Mitogenomes (synonym mitochondrial genomes) are useful molecular markers for analyzing population structure, phylogenetic relationships and divergence time (*Igawa et al., 2008*; *Masta et al., 2002*) due to their small size, lack of recombination, rapid evolution rate, conserved gene content and genomic organization, and maternal inheritance (*Masta et al., 2002*; *Zhang et al., 2003*). In addition, mitogenomes have high substitution rates and these substitutions may have relevant effects on fitness and metabolism (*Carapelli et al., 2019*). Although mitogenomes are usually thought to be under neutral or nearly neutral selection, evidence has accumulated for positive selection acting on mitochondrial genes associated with environmental adaptations (*Carapelli et al., 2019*; *Shen et al., 2010*). Hence, the mitogenome is a likely target for environmental selection and it is useful in analyzing positive selection or natural selection (*Zhou et al., 2014*).

Mitochondria are called the powerhouses of the cell because they synthesize most of the ATP necessary to drive cell functions (*McBride, Neuspiel & Wasiak, 2006*). Numerous environmental factors can affect the growth and survival of amphibians, including temperature and salinity (*Yaghobi et al., 2018*). Temperature has a great effect on the bioenergetic demands and metabolic adaptation of ectotherms (*Sun et al., 2018a*). For

example, negative selection was found in the mitochondrial protein-coding genes of *Glandirana* (*Xia et al., 2014*). *Malyarchuk et al. (2010)* postulated that the amino acid changes in cytochrome B (*CYTB*) might be advantageous in cold climatic conditions and make it possible for several Siberian salamanders to live in extreme cold environments. Adaptation to saline environments probably needs more energy devoted to osmoregulation (*Xia et al., 2017*) and several genes in the mitogenome appear to be under positive selection for the role that they play in energy metabolism (*Caballero et al., 2015*). Salinity and osmoregulation are also significant factors in the survival and fitness of all amphibians because their skin is highly water-permeable (*Yaghobi et al., 2018*). Indeed, *Whitehead (2009)* found that salinity differences were associated with amino acid changes in the mitochondrial protein-coding genes of *Fundulus* fish populations along the Atlantic coast.

Mitogenomes could have an impact on energy metabolism, thermoregulation and osmoregulation. However, few studies of Anura have examined the potential involvement of mitogenome adaptations to life in extreme environments. *Anaxyrus americanus* (synonym *Bufo americanus*) is a small American toad (*Frost et al., 2006*; *Masta et al., 2002*). It is widely distributed across North America (*Haislip et al., 2011*) and can live in places with low nighttime temperatures below 0 °C for as much as eight months of the year. However, contrary to various frog species in the same environment that endure whole body freezing in winter (*Storey & Storey, 2017*), *A. americanus* is freeze intolerant (*Bergstrom, 2010*; *Storey & Storey, 1986*) and typically overwinters by digging underground to below the frostline. *Bufotes pewzowi* (synonym *Bufo pewzowi*) is distributed in China, Kazakhstan, Kyrgyzstan, Mongolia and Uzbekistan; belonging to the *Bufo viridis* group, the species can withstand low temperatures and a high level of water salinity (*Katz et al., 1981*; *Ren et al., 2009*). Hence, we hypothesized that the mitogenome adaptations of these two species that live in low temperature (*A. americanus*) or low temperature and high water salinity (*Bufotes pewzowi*) environments may be affected by these extreme environments. Therefore, in the present study, we sequenced and annotated the complete mitogenomes of *A. americanus* and *Bufotes pewzowi*, these being the first reported mitogenomes for the genera *Anaxyrus* and *Bufotes*, and clarified their mitogenome differences and similarities in comparison with other Bufonidae species. We also performed evolutionary relationship analyses to discuss the intergeneric relationships among the Bufonidae and evaluated potential positive selection in *A. americanus* and *Bufotes pewzowi* by using the branch model and the site model. These two complete mitogenomes represent two genera for which complete mitogenomes were previously unknown. Hence, our results not only supplement the limited molecular data previously available for Bufonidae, but also examine the monophyly of Bufonidae and explore the idea of adaptive evolution of mitogenomes in response to extreme environmental stresses.

MATERIALS AND METHODS

Sample Collection and DNA extraction

The specimens of *A. americanus* and *Bufotes pewzowi* were collected in Ottawa, Ontario, Canada (45°25.38′N, 75°43.11′W) and Aksu, Xinjiang, China (41°10.54′N, 80°16.81′E),

respectively. Both were identified by J.Y. Zhang. Toe-clip samples of both species were stored at −80 °C in the Institute of Ecology, Zhejiang Normal University. Our experimental procedures complied with the current regulations on animal welfare and research in China and Canada. The Animal Research Ethics Committees of Zhejiang Normal University and Carleton University approved the experimental design (No.1082196).

PCR amplification, and sequencing

Total DNA was extracted from the toe-clips samples of *A. americanus* or *Bufotes pewzowi* using an Ezup Column Animal Genomic DNA Purification Kit (Sangon Biotech Company, Shanghai, China). The 11 universal primers for standard polymerase chain reaction (PCR) amplification of mitogenomes were slightly modified according to *Yu et al. (2015)* and *Zhang et al. (2013)* and 15 specific primers were designed based on the sequenced fragments from universal primers using Primer Premier 5.0 (PREMIER Biosoft International, CA, USA) (Tables S1 and S2). All PCR amplifications were carried out in a 50 µL reaction mixture and the procedures were performed using an Eppendorf Thermal Cycler (Mastercycle® nexus GSX1, Hamburg, Germany). We used both standard PCR and Long-PCR methods with *TaKaRa Ex-Taq* and *TaKaRa LA-Taq Kits* (Takara Biomedical, Dalian, China). These two methods were slightly modified from *Yu et al. (2015)* and *Zhou et al. (2009)*. All PCR products were detected by electrophoresis on 1% agarose gels, and sequences were obtained in an automated DNA sequencer (ABI 3730) by Sangon Biotech Company (Shanghai, China).

Mitogenome annotation and sequence analyses

Sequences were checked and assembled using SeqMan (Lasergene version 5.0) (*Burland, 2000*). The 22 tRNAs were identified by their cloverleaf secondary structure using tRNAscan SE 1.21 (*Lowe, 1997*) (http://lowelab.ucsc.edu/tRNAscan-SE/) or determined by comparison with the available tRNA genes of closely related anurans downloaded from GenBank. Location of the 13 PCGs and 2 rRNA genes were determined by comparison with homologous sequences of mtDNA from other Bufonidae species using ClustalW (*Thompson, Higgins & Gibson, 1994*) and then PCGs were checked and translated to amino acids using the vertebrate mitogenome code by Mega 5.0 (*Tamura et al., 2011*). The mitogenome maps of *A. americanus* and *Bufotes pewzowi* were constructed using GenomeVx (http://wolfe.gen.tcd.ie/GenomeVx/) (*Conant & Wolfe, 2008*). The A+T and C+G content values, codon usage and relative synonymous codon usage (RSCU) of protein-coding genes were calculated using Mega 5.0 (*Tamura et al., 2011*). Nucleotide sequence skewness was calculated according to the following formulae: AT-skew = (A −T)/(A +T) and GC-skew = (G −C)/(G +C) (*Perna & Kocher, 1995*).

Phylogenetic analyses

To confirm the phylogenetic relationships among Bufonidae, 19 sequences of complete or partial mitochondrial genomes were used. The data set was inclusive of the ingroups of the 2 species from this study, 13 other species from Bufonidae (*Cao et al., 2006*; *Dong & Yang, 2016*; *Igawa et al., 2008*; *Jacob Machado et al., 2018*; *Jiang et al., 2017b*; *Machado, Lyra & Grant, 2016*; *Wang et al., 2013*; *Yang et al., 2016*; *Zhang et al., 2005*; *Zhang et al., 2013*) and

Table 1 GenBank accession numbers of the species used in constructing the phylogenetic trees.

Family	Genus	Species	GenBank accession number	References
	Anaxyrus	*Anaxyrus americanus*	MK855099	
		Bufo japonicus	AB303363.1	*Igawa et al. (2008)*
		Bufo gargarizans	DQ275350.1	*Cao et al. (2006)*
	Bufo	*Bufo tibetanus*	JX878885.1	*Wang et al. (2013)*
		Bufo stejnegeri	KR136211.1	*Dong & Yang (2016)*
		Bufo gargarizans minshanicus	KM587710.1	*Yang et al. (2016)*
Bufonidae		*Bufo gargarizans*	KU321581.1	*Jiang et al. (2017a)* and *Jiang et al. (2017b)*
	Bufotes	*Bufotes pewzowi*	MK855100	
	Duttaphrynus	*Bufo melanostictus*	AY458592.1	*Zhang et al. (2005)*
	Leptophryne	*Leptophryne borbonica*	JX564876.1	*Zhang et al. (2013)*
	Melanophryniscus	*Melanophryniscus moreirae*	KY962391.1	*Jacob Machado et al. (2018)*
		Melanophryniscus simplex	KT221611.1	*Machado, Lyra & Grant (2016)*
	Rhinella	*Rhinella sp.*	KT221613.1	*Machado, Lyra & Grant (2016)*
Aromobatidae	*Mannophryne*	*Mannophryne trinitatis*	JX564878.1	*Zhang et al. (2013)*
		Dendrobates tinctorius	MF069441.1	*Lyra et al. (2017)*
Dendrobatidae	*Dendrobates*	*Dendrobates leucomelas*	MF069436.1	*Lyra et al. (2017)*
		Dendrobates auratus	MF069434.1	*Lyra et al. (2017)*

the outgroups of 4 species from *Mannophryne* and *Dendrobatidae* (*Lyra et al., 2017*; *Zhang et al., 2013*). Accession numbers of all mitogenomes are summarized in Table 1. The amino acid and nucleotide sequences of the 13 protein-coding genes from all 19 species were employed to construct BI and ML phylogenetic trees according to the methods of *Zhang et al. (2018)* and *Zhou et al. (2009)*. All of the 13 PCGs were aligned using Clustal W in Mega 5.0 (*Tamura et al., 2011*) and were analyzed with Gblocks 0.91b (*Castresana, 2000*) using default settings to select conserved regions. The best partition scheme and evolutionary model were determined with the PartitionFinder v.1.1.1 program (*Lanfear et al., 2012*), using the Bayesian Information Criterion (BIC) (*Schwarz, 1978*). For the ML analysis, we used the RAxML program (*Stamatakis, 2014*) under the GTRGAMMAI model with 1,000 bootstrap replications. For BI analysis, we used MrBayes 3.1.2 (*Huelsenbeck & Ronquist, 2001*) under the GTR+I+G model. Markov Chain Monte Carlo (MCMC) was run with four chains for 10 million generations, with sampling every 1,000 generations. The first 25% of generations were removed as burn-in, which was decided by checking convergences of -log likelihood (*-lnL*). After the average standard deviation of split frequencies in Bayesian was below 0.01, we judged that the Bayesian analysis had reached sufficient convergence.

Analysis of positive selection

The program EasyCodeML (*Gao et al., 2019*) was used to analyze the selective pressure on mitogenomes; this is an interactive visual tool for detecting selection in a molecular evolutionary analysis based on CodeML (*Yang, 2007*). The ω ratio is the rate of nonsynonymous (dN) versus synonymous (dS) substitution (dN/dS) and can indicate natural selection acting on the proteins. All of the concatenated 13 PCGs (Table S3) were

used in the analysis and the values for ω ratio >1, =1 or <1 indicate positive selection, neutral evolution or negative selection, respectively (*Yang, 2007*). To investigate whether positive selection occurred on specific branches, branch models were run under the one-ratio model (M0) or the two-ratio model with *A. americanus* or *Bufotes pewzowi* as the foreground branch, respectively. M0 assumes that all branches have the same ω ratio values whereas the two-ratio model assumes one ω ratio value for the branches of interest and the other for the background branches. Because different topologies of trees will affect the results, both of the phylogenetic trees structured in BI and ML were used in the analyses. In addition, a likelihood ratio test (LRT) was performed to assess the significant difference between the results of the M0 and the two-ratio model (*Yu et al., 2011*). Variation happens mostly in several base pairings and may affect a few sites in some lineages (*Yang, 2007*; *Yu et al., 2011*). Consequently, the site model was applied to detect the potential selection among sites and allow for different ω ratios in different sites, codons or amino acids (*Yang, 2007*). Seven useful codon substitution models were taken into account in the calculations, including M0 (one ratio), M1a (Nearly Neutral), M2a (Positive Selection), M7 (β), M8 (β & ω) and M8a (β & $\omega = 1$). We also used LRTs to assess these models and Bayes Empirical Bayes (BEB) to evaluate the posterior probability of positive selection sites. The three-dimensional (3D) structures of the amino acid positive selections in the ND6 protein were formed using SWISS-MODEL Workspace (*Waterhouse et al., 2018*).

RESULTS AND DISCUSSION

Mitogenome organization and arrangement

The lengths of the complete *A. americanus* and *Bufotes pewzowi* mitogenomes are 17,328 base pairs (bp) and 17,551 bp, respectively (Table 2). Both mitogenomes are circular and contain the typical 37 genes (Tables 3 and 4). Most of the genes are coded on the H-strand, except for 8 tRNA genes and the *ND6* gene on the L-strand. Gene structures are detailed in Figs. 1 and 2. In addition, the gene order and composition are identical with that of other mitogenomes of Bufonidae (*Dong & Yang, 2016*; *Jiang et al., 2017b*; *Zhang et al., 2016*). The different lengths of the mitogenomes are primarily caused by the different sizes of intergenic nucleotides (IGNs) (Tables 3 and 4), particularly the length of the CRs. The overall base composition, A+T and G+C content, as well as AT and GC skew of the *A. americanus* and *Bufotes pewzowi* genomes are listed in Table 2; these data show that *A. americanus* has the highest A+T content (62.4%) and a strong A+T bias. The H-strand of both mitogenomes showed a negative AT-skew and GC-skew, which is expected for most vertebrates (*Fonseca, Froufe & Harris, 2006*; *Hao, Ping & Zhang, 2016*; *Zhang et al., 2019*). Previous studies showed that the asymmetry of the nucleotides resulted primarily from mutations affecting the H-strand during its single-stranded state (*Sahyoun et al., 2014*).

Protein-coding genes and codon usages

All the typical 13 PCGs ranged from 165 bp (*ATP8*) to 1,789 bp (*ND5*) in both *A. americanus* and *Bufotes pewzowi*. In addition, the total size of the 13 PCGs in *A. americanus* and *Bufotes pewzowi* were identical (11,290 bp). Mitochondrial PCGs have no introns, but have several

Table 2 The mitogenome composition of *A. americanus* and *Bufotes pewzowi*.

Region	Size (bp)		A+T content		C+G content		AT-skew		CG-skew	
	A. americanus	*B. pewzowi*	*A. americanus*	*B. pewzowi*	*A. americanus*	*B. pewzowi*	*A. americanus*	*B. pewzowi*	*A. americanus*	*B. pewzowi*
Whole Genome	17,328	17,551	62.4	59.1	37.6	40.9	−0.038	−0.002	−0.248	−0.271
PCGs	11,290	11,290	61.9	58.6	38	41.5	−0.111	−0.085	−0.256	−0.272
rRNA	2,536	2,543	60.7	58.8	39.4	41.2	0.117	0.149	−0.086	−0.103
tRNA	1,534	1,535	58.9	59.5	41.2	40.4	0.039	0.028	0.014	0.04
CRs	1,916	2,129	70.3	63	29.7	37.1	−0.030	0.006	−0.205	−0.294

Table 3 The mitogenome gene characteristics and location of [i] *A. americanus*.

Gene	Strand	Position	Length (nuc.)	Anticodon	Start codon	Stop codon	Intergenic nucleotides
tRNA^{Leu}	+	1–72	72	TAG			0
tRNA^{Thr}	+	73–144	72	TGT			0
tRNA^{Pro}	−	144–212	69	TGG			−1
tRNA^{Phe}	+	212–279	68	GAA			−1
12S rRNA	+	280–1213	934				0
tRNA^{Val}	+	1214–1282	69	TAC			0
16S rRNA	+	1283–2884	1602				0
tRNA^{Leu}	+	2885–2957	73	TAA			0
ND1	+	2958–3918	961		TTG	T	0
tRNA^{Ile}	+	3919–3989	71	GAT			0
tRNA^{Gln}	−	3989–4059	71	TTG			−1
tRNA^{Met}	+	4059–4127	69	CAT			−1
ND2	+	4128–5162	1035		ATT	TAG	0
tRNA^{Trp}	+	5161–5230	70	TCA			−2
tRNA^{Ala}	−	5232–5300	69	TGC			+1
tRNA^{Asn}	−	5302–5374	73	GTT			+1
L-strand origin of replication		5375–5403	29				0
tRNA^{Cys}	−	5401–5464	64	GCA			−3
tRNA^{Tyr}	−	5465–5534	70	GTA			0
COX1	+	5539–7080	1542		ATA	TAA	+4
tRNA^{Ser}	−	7081–7151	71	TGA			0
tRNA^{Asp}	+	7156–7224	69	GTC			+4
COX2	+	7226–7910	685		ATG	T	+1
tRNA^{Lys}	+	7911–7982	73	TTT			0
ATP8	+	7984–8148	165		ATG	TAA	+1
ATP6	+	8139–8822	684		ATG	TAA	−10
COX3	+	8822–9605	784		ATG	T	−1
tRNA^{Gly}	+	9606–9674	69	TCC			0
ND3	+	9675–10016	340		ATG	T	0
tRNA^{Arg}	+	10015–10083	69	TCG			0
ND4L	+	10084–10383	300		ATG	TAA	0
ND4	+	10377–11741	1365		ATG	TAA	−7
tRNA^{His}	+	11742–11810	69	GTG			0
tRNA^{Ser}	+	11811–11877	67	GCT			0
ND5	+	11915–13703	1789		ATG	T	+37
ND6	−	13701–14195	495		ATG	AGA	−3
tRNA^{Glu}	−	14196–14263	68	TTC			0
CYTB	+	14269–15411	1143		ATG	AGG	+5
control region		15412–17328	1917				0

Table 4 The mitogenome gene characteristics and location of *Bufotes pewzowi*.

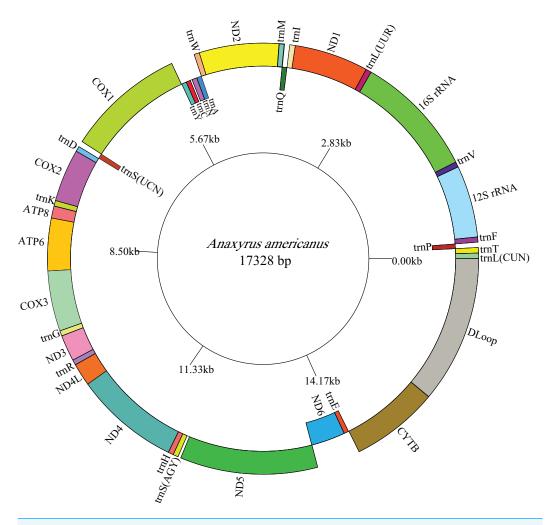| Gene	Strand	Position	Length (nuc.)	Anticodon	Start codon	Stop codon	Intergenic nucleotides
tRNA^{Leu}	+	1–72	72	TAG			0
tRNA^{Thr}	+	73–144	72	TGT			0
tRNA^{Pro}	−	144–212	69	TGG			−1
tRNA^{Phe}	+	212–279	68	GAA			−1
12S rRNA	+	280–1213	934				0
tRNA^{Val}	+	1214–1282	69	TAC			0
16S rRNA	+	1283–2891	1609				0
tRNA^{Leu}	+	2892–2964	73	TAA			0
ND1	+	2965–3925	961		TTG	T	0
tRNA^{Ile}	+	3926–3996	71	GAT			0
tRNA^{Gln}	−	3996–4066	71	TTG			−1
tRNA^{Met}	+	4066–4134	69	CAT			−1
ND2	+	4135–5169	1035		ATT	TAG	0
tRNA^{Trp}	+	5168–5237	70	TCA			−2
tRNA^{Ala}	−	5238–5306	69	TGC			0
tRNA^{Asn}	−	5307–5379	73	GTT			0
L-strand origin of replication		5380–5407	28				0
tRNA^{Cys}	−	5405–5468	64	GCA			−3
tRNA^{Tyr}	−	5469–5538	70	GTA			0
COX1	+	5543–7084	1542		ATA	TAA	+4
tRNA^{Ser}	−	7087–7157	71	TGA			+2
tRNA^{Asp}	+	7159–7227	69	GTC			+1
COX2	+	7229–7916	688		ATG	T	+1
tRNA^{Lys}	+	7917–7988	72	TTT			0
ATP8	+	7990–8154	165		ATG	TAA	+1
ATP6	+	8151–8828	678		ATA	TAA	−4
COX3	+	8828–9611	784		ATG	T	−1
tRNA^{Gly}	+	9612–9680	69	TCC			0
ND3	+	9681–10022	342		ATG	TAA	0
tRNA^{Arg}	+	10021–10089	69	TCG			−2
ND4L	+	10090–10389	300		ATG	TAA	0
ND4	+	10383–11747	1365		ATG	TAA	−7
tRNA^{His}	+	11748–11816	69	GTG			0
tRNA^{Ser}	+	11817–11883	67	GCT			0
ND5	+	11923–13711	1789		ATG	T	+39
ND6	−	13709–14203	495		ATG	AGG	−3
tRNA^{Glu}	−	14204–14272	69	TTC			0
CYTB	+	14277–15422	1146		ATG	AGA	+4
control region		15423–17551	2129				0

Figure 1 Mitogenome map of *A. americanus*. The one-letter amino acid codes are used to label the tR-NAs. Gene names on the inside indicate that the direction of transcription is from left to right, whereas gene names on the outside indicate right to left transcription.

Full-size ⬚ DOI: 10.7717/peerj.8901/fig-1

overlapping nucleotides with the adjacent gene. There are 5 and 6 reading frame overlaps in the mitogenome of *A. americanus* and *Bufotes pewzowi*, respectively (Tables 3 and 4). All PCGs begin with ATA or ATG as the start codons, except *ND1* that begins with TTG. Although TTG is an uncommon start codon among PCGs, it is often found in amphibians (*Wang, Cao & Li, 2017*; *Zhang et al., 2005*). The stop codons for *A. americanus* and *Bufotes pewzowi* are mostly complete TAA, AGG, AGA, and TAG codons with some incomplete T codons. The functionality of these latter is believed to be restored by post-transcriptional polyadenylation (*Liu, Wang & Su, 2005*; *Ojala, Montoya & Attardi, 1981*). Furthermore, a comparative analysis indicated that the mitogenome of *A. americanus* had the highest A+T content (61.9%) (*Dong & Yang, 2016*; *Jacob Machado et al., 2018*). We also analyzed the relative synonymous codon usage (RSCU) of the *A. americanus* and *Bufotes pewzowi* mitogenomes, excluding stop codons (Table 5; Figs. 3 and 4). The results show that A and T at the third codon position are slightly overused when compared to the synonymous
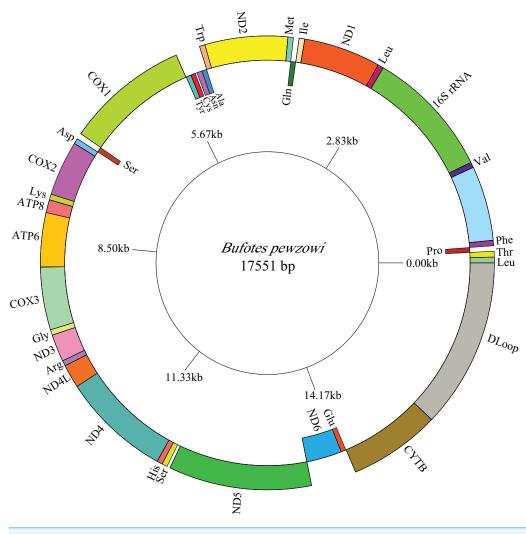
Figure 2 **Mitogenome map of *B. pewzowi*.** The one-letter amino acid codes are used to label the tRNAs. Gene names on the inside indicate that the direction of transcription is from left to right, whereas gene names on the outside indicate right to left transcription.

Full-size 🖼 DOI: 10.7717/peerj.8901/fig-2

codons of C and G. Moreover, we found that the most frequently used amino acids in these two mitogenomes are *Leu* (CUN), *Ile* and *Ala*, with those encoding *Cys* and *Ser* (AGY) being rare.

Ribosomal and transfer RNA genes

We found that the length of rRNAs in *Bufotes pewzowi* (2,543 bp) is longer than other Bufonidae species (*Cao et al., 2006*; *Igawa et al., 2008*; *Jiang et al., 2017b*; *Wang et al., 2013*; *Yang et al., 2016*). The complete mitogenome of *A. americanus* or *Bufotes pewzowi* contains 22 typical tRNA genes, which ranged from 64 bp to 73 bp in length. In the H-strand, *A. americanus* showed a positive AT-skew and GC-skew of the tRNAs, and *Bufotes pewzowi* also showed a positive AT-skew and GC-skew (Table 2). Furthermore, all of the tRNA genes displayed the potential to fold into the typical cloverleaf secondary structure, excluding

Cai et al. (2020), *PeerJ*, DOI 10.7717/peerj.8901

12/28

Table 5 **RSCU information for the mitochondrial protein-coding genes of *A. americanus* and *Bufotes pewzowi*.**

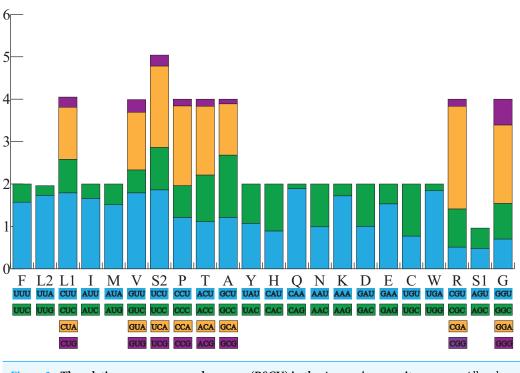| Codon	A. americanus		B. pewzowi		Codon	A. americanus		B. pewzowi		Codon	A. americanus		B. pewzowi		Codon	A. americanus		B. pewzowi	
	Count	RSCU	Count	RSCU		Count	RSCU	Count	RSCU		Count	RSCU	Count	RSCU		Count	RSCU	Count	RSCU
UUU(F)	202	1.57	168	1.3	UCU(S2)	93	1.86	67	1.36	UAU(Y)	58	1.07	56	1	UGU(C)	12	0.77	10	0.71
UUC(F)	55	0.43	90	0.7	UCC(S2)	50	1	65	1.32	UAC(Y)	50	0.93	56	1	UGC(C)	19	1.23	18	1.29
UUA(L2)	176	1.73	130	1.3	UCA(S2)	96	1.92	105	2.13	UAA(*)	5	2.5	6	2.67	UGA(W)	103	1.84	96	1.73
UUG(L2)	23	0.23	28	0.28	UCG(S2)	13	0.26	14	0.28	UAG(*)	1	0.5	1	0.44	UGG(W)	9	0.16	15	0.27
CUU(L1)	182	1.79	144	1.44	CCU(P)	61	1.21	47	0.94	CAU(H)	38	0.89	31	0.7	CGU(R)	9	0.51	10	0.57
CUC(L1)	80	0.79	110	1.1	CCC(P)	38	0.75	50	1	CAC(H)	47	1.11	58	1.3	CGC(R)	16	0.9	10	0.57
CUA(L1)	125	1.23	151	1.51	CCA(P)	95	1.88	89	1.78	CAA(Q)	83	1.89	76	1.67	CGA(R)	43	2.42	45	2.57
CUG(L1)	24	0.24	37	0.37	CCG(P)	8	0.16	14	0.28	CAG(Q)	5	0.11	15	0.33	CGG(R)	3	0.17	5	0.29
AUU(I)	281	1.66	214	1.32	ACU(T)	78	1.11	66	0.93	AAU(N)	67	0.99	61	0.92	AGU(S1)	24	0.48	10	0.2
AUC(I)	57	0.34	111	0.68	ACC(T)	77	1.1	99	1.39	AAC(N)	68	1.01	72	1.08	AGC(S1)	24	0.48	35	0.71
AUA(M)	131	1.51	116	1.35	ACA(T)	114	1.62	108	1.52	AAA(K)	73	1.72	74	1.68	AGA(*)	1	0.5	1	0.44
AUG(M)	42	0.49	56	0.65	ACG(T)	12	0.17	11	0.15	AAG(K)	12	0.28	14	0.32	AGG(*)	1	0.5	1	0.44
GUU(V)	83	1.79	75	1.55	GCU(A)	92	1.21	83	1.06	GAU(D)	37	1	29	0.77	GGU(G)	39	0.7	37	0.66
GUC(V)	25	0.54	36	0.75	GCC(A)	111	1.47	123	1.57	GAC(D)	37	1	46	1.23	GGC(G)	47	0.84	56	1
GUA(V)	63	1.36	56	1.16	GCA(A)	92	1.21	96	1.22	GAA(E)	71	1.53	63	1.4	GGA(G)	103	1.85	80	1.43
GUG(V)	14	0.3	26	0.54	GCG(A)	8	0.11	12	0.15	GAG(E)	22	0.47	27	0.6	GGG(G)	34	0.61	51	0.91

Figure 3 **The relative synonymous codon usage (RSCU) in the *A. americanus* mitogenome.** All codons used as well as the different combinations of synonymous codons are listed on the x-axis, whereas RSCU values are listed on the *y*-axis. Each amino acid is replaced by one letter, except for Leu and Ser which have two abbreviations because they have two different codons.

the *trnC* and *trnS* (AGY) (Figs. S1 and S2). In both species, the *trnS* (AGY) has an extra unpaired adenine (A) in the anticodon arm and the *trnC* has lost the DHU loop. This phenomenon is also found in other Bufonidae species (shown in Fig. S3) (*Cao et al., 2006*; *Igawa et al., 2008*; *Zhang et al., 2005*; *Zhang et al., 2013*). The *trnS* (AGY) in *A. americanus* had also lost the DHU arm, whereas in *Bufotes pewzowi* lost only the DHU loop. Hence, the unusual secondary structure of *trnS* (AGY) is in line with the molecular trend observed in metazoa (*Wolstenholme, 1992*). We also found 13 unmatched base pairs in *A. americanus* and 15 in *Bufotes pewzowi*. The putative origin of L-strand replications (O_L) are 29 bp and 28 bp long in *A. americanus* and *Bufotes pewzowi*, respectively. Both of these have the potential to fold into the characteristic stem and loop structure (*Jiang et al., 2017a*; *Sahyoun et al., 2014*) that has been demonstrated by *Hixson & Brown (1986)* to be involved in the transition from RNA to DNA synthesis.

Control region and intergenic regions

The control regions (CRs) in *A. americanus* and *Bufotes pewzowi* have lengths of 1,916 bp and 2,129 bp, respectively. The A+T content value (70.3%) of *A. americanus* is the highest known to date among Bufonidae species. In addition, *A. americanus* showed a negative AT-skew and GC-skew in its CR, whereas *Bufotes pewzowi* showed a positive AT-skew and negative GC-skew. Guanine (G) was the scarcest nucleotide at the third codon position of the H-strand due to a strong bias against guanine usage in the *A. americanus* mitogenome,
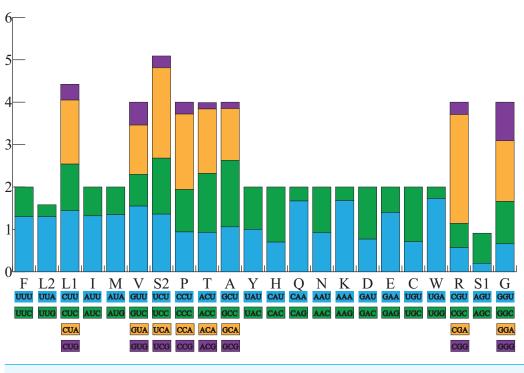
Figure 4 **The relative synonymous codon usage (RSCU) in the *B. pewzowi* mitogenome.** All codons used as well as the different combinations of synonymous codons are listed on the *x*-axis, whereas RSCU values are listed on the y-axis. Each amino acid is replaced by one letter, except for Leu and Ser which have two abbreviations because they have two different codons.

Full-size ⬜ DOI: 10.7717/peerj.8901/fig-4

which is common for mitogenome strands of vertebrates (*Kan et al., 2010*). The CRs can be divided into three regions that depend on the distribution of the variable nucleotide positions and differential frequencies of the nucleotides, and contain repeat regions at both 5′ and 3′-sides. We found 3 tandem repeats in *A. americanus* with consensus sizes of 162 bp, 21 bp and 2 bp. In *Bufotes pewzowi* there are only two tandem repeats whose consensus sizes were 104 bp and 91 bp. The intergenic spacers (IGNs) have a variable length within the mitogenomes of *A. americanus* (Table 3) and *Bufotes pewzowi* (Table 4). All lengths of IGNs in both species are smaller than 5 bp, except for one that was 37 bp in *A. americanus* and 39 bp in *B. pewzowi*, both located between the *trnS* (AGY) and *ND5* genes. Comparative analysis showed that the longest IGN between *A. americanus* and *Bufotes pewzowi* had a high similarity (76.9%). In many vertebrates, there is usually a *trnL* (CUN) gene following the *trnS* (AGY) gene (*Cheng et al., 2018*; *Lin et al., 2014*; *Ni et al., 2016*; *Ye et al., 2016*; *Yu et al., 2012*; *Yu, Zhang & Zheng, 2012*). However, when the *trnL* (CUN) gene is translocated, an IGN is left in its original position (*Zhou et al., 2009*). Thus, *Cao et al. (2006)* speculated that this might reflect the evolution of the mitogenome arrangement in Anura.

Phylogenetic analyses
Phylogenetic relationships based on the nucleotide sequences of the 13 PCGs were obtained with BI and ML analyses (Fig. 5). Our BI analysis was relatively robust and provided resolution with high clade posterior probabilities, whereas the ML results showed some
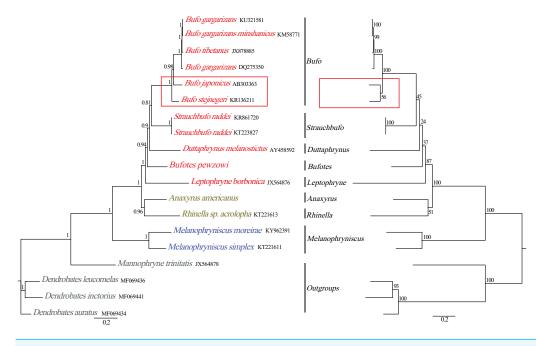
Figure 5 **Phylogenetic relationships among Bufonidae in BI and ML analyses.** The BI analysis result is shown on the left and the numbers above the nodes are posterior probability. The ML analysis is on the right and the numbers above the nodes are bootstrap value.

Full-size ⬚ DOI: 10.7717/peerj.8901/fig-5

modest clade frequencies. Furthermore, the phylogenetic relationships deduced from BI and ML analyses showed somewhat different topologies. In the BI and ML analyses, the monophyly of Bufonidae was well recovered. In the BI analysis, *Bufo japonicus* was a sister group to the clade of (*Bufo gargarizan* DQ275350 + (*Bufo tibetanus* JX878885 + (*Bufo gargarizan* KM587710 + *Bufo gargarizan* KU321581))). However, in the ML analysis, *Bufo japonicus* was a sister group to *Bufo stejnegeri* and then the group of (*Bufo japonicus* + *Bufo stejnegeri*) was a sister group to the cluster of (*Bufo gargarizan* DQ275350 + (*Bufo tibetanus* JX878885 + (*Bufo gargarizan* KM587710 + *Bufo gargarizan* KU321581))). Coincidentally, *Dong & Yang (2016)* also reported that *Bufo japonicus* was a sister group to *Bufo stejnegeri* and the monophyly of family Bufonidae and genus *Bufo* were corroborated. *Frost et al. (2006)* and *Van Bocxlaer et al. (2009)* corroborated the monophyly of Bufonidae as well as the results of *Portik & Papenfuss (2015)*. Our phylogeny within Bufonidae is generally similar to the results of *Pramuk et al. (2008)*, *Ron et al. (2015)* and *Dong & Yang (2016)*. The ML and BI analyses also confirmed the monophyly of *Bufo*, which has also been demonstrated by other researchers (*Graybeal, 1997*; *Dong & Yang, 2016*). By contrast, our results were different from *Brandvain et al. (2014)* and *Jiang et al. (2018)*, who reported that *Bufo* was a paraphyletic group, a result that was also deduced by *Pyron & Wiens (2011)*. However, we found that *Dong & Yang (2016)* confirmed the monophyly of *Bufo* using the complete mitogenomes, whereas *Brandvain et al. (2014)*, *Pyron & Wiens (2011)* and *Jiang et al. (2018)* confirmed a paraphyletic relationship using partial mitochondrial genes (*12S*,

16S and *CYTB*) and several nuclear genes. Hence, the different results from these studies are likely caused by the different data sets and/or methods applied.

The family Bufonidae was divided into 3 major groups: (*Leptophryne* + (*Bufotes* + (*Duttaphrynus* + (*Strauchbufo* + (genus *Bufo*))))), (*A. americanus* + *Rhinella acrolopha*), and (*Melanophryniscus simplex* + *M. moreirae*). Among them, the clade of *A. americanus* was the sister group to *R. acrolopha* whereas *Bufotes pewzowi* was a sister group to the clade of (*Duttaphrynus* + (*Strauchbufo* + (genus *Bufo*))). Genus *Anaxyrus* was a sister group to genus *Rhinella* and then the clade of (*A. americanus* + *R. acrolopha*) was the sister group to (*Leptophryne* + (*Bufotes* + (*Duttaphrynus* + (*Strauchbufo* + (*Bufo*))))). *Portik & Papenfuss (2015)* also found that genus *Anaxyrus* was the sister group to genus *Rhinella*. Our phylogenetic tree showed that the clade of (*M. simplex* + *M. moreirae*) (BI: 1, ML: 100%) was recovered as the sister group to the other Bufonidae species. We also found a similar result in the research of *Portik & Papenfuss (2015)*. The South American genera include *Melanophryniscus*, *Nannophryne*, as well as the group of *Rhinella* that is endemic to South America and is distributed from the southern tip of Texas to as far south as Argentina (*Vallinoto et al., 2010*). This phenomenon was consistent with the results from other researchers and implies that Bufonidae may have originated from South America. Coincidentally, nearly all recent phylogenetic analyses have asserted a South American origin for Bufonidae (*Pérez-Ben, Gómez & Báez, 2019*; *Pramuk et al., 2008*). In addition, discrepancies in the results between our work and prior studies were likely to be caused by the different composition of the data chosen (*Gao et al., 2018*). Therefore, more molecular data are needed to better comprehend the phylogenetic relationship of the family, especially from taxa that, in other studies, led to a conclusion that *Bufo* was paraphyletic.

Analysis of positive selection in 13 protein-coding genes

The results of positive selection are shown in Tables 6 and 7. In the analyses of the branch model, we reached a similar conclusion no matter which toad species was set as the foreground branch. The ω ratio value in the M0 model was 0.03375 when using the BI tree and 0.03373 using the ML tree, with ω ratio values all smaller than 1. This means that these two branches are under negative selection. When we set *A. americanus* as the foreground branch, the LRT of the comparison (M0 vs. the two-ratio model) was highly significant ($p < 0.01$), whereas when *Bufotes pewzowi* was set as the foreground branch, the LRT value was greater than 0.05. The site model was used to detect positive selection sites and we got similar conclusions regardless of which tree-building method was used. The LRT of M7-M8 comparison showed high significance ($P < 0.01$) and two amino acid positions were found have BEB values >0.90 (positions 3,590 and 3,594 in the concatenated amino acids of the 13 PCGs). Amino acid residues 3,590 and 3,594 correspond to amino acid positions 115 and 119 in the ND6 protein, respectively (Table S3). Residue glycine (G, 115) in the ND6 protein can be found in *A. americanus*, *Bufo gargarizan*, *Bufo japonicus*, *Bufo stejnegeri*, *Bufo tibetanus* and *S. raddei*, which are distributed across northern regions of the earth at similar latitudes (33°N to 44°N), and residues serine as well as glutamic acid can also be found in this position in other Bufonidae. Residue aspartic acid (D, 119) in the ND6 protein can only be found in *A. americanus* whereas most of the other Bufonidae species contain glycine

Table 6 Summary of EasyCodeML analysis of positive selection on mitogenomes based on the phylogenetic tree from BI.

Foreground branch	Models	ℓn L	Estimates of parameters	Model compared	LRT *P*-value	Positive sites
Branch model						
A. americanus	M0	−64953.9215	$\omega = 0.03375$	M0 vs. two-ratios model	0.000000011	
	two-ratios model	−64937.6024	$\omega 0 = 0.03520, \omega 1 = 0.01846$			
Bufotes pewzowi	M0	−64953.9215	$\omega = 0.03375$	M0 vs. two-ratios model	0.588391030	
	two-ratios model	−64953.7750	$\omega 0 = 0.03390, \omega 1 = 0.03200$			
Site model						
	M0	−64953.9215	$\omega 0 = 0.03375$			
	M3	−63675.0885	$\omega 0 = 0.00589, \omega 1 = 0.1673, \omega 2 = 101.4548$ p0=0.8120, p1=0.1880, p2=0.00000	M0 vs. M3	0.000000000	[] Not Allowed
	M1a	−64441.3475	$\omega 0 = 0.02382, \omega 1 = 1.00000$ p0=0.9533, p1=0.04670	M1a vs. M2a	0.999999000	[] Not Allowed
	M2a	−64441.3475	$\omega 0 = 0.02382, \omega 1 = 1.0000, \omega 2 = 40.4741$ p0=0.9533, p1=0.04670, p2=0.0000			
	M7	−63769.6465	$p = 0.1688, q = 2.4104$	M7 vs.M8	0.000000000	3584 I 0.655, 3585 T 0.654, 3590 G 0.925, 3594 D 0.942 Not Allowed
	M8	−63735.9750	$\omega 0 = 1.00000, q = 2.5906$ p0=0.9893, p1=0.01066, p2=0.1583			
	M8a	−63639.2914	$\omega 0 = 1.00000, q = 3.8610$ p0=0.9985, p1=0.00149, p2=0.1657	M8a vs.M8	0.000000000	Not Allowed

Table 7 Summary of EasyCodeML analysis of positive selection on mitogenomes based on the maximum-likelihood tree.

Foreground branch	Models	ℓn L	Estimates of parameters	Model compared	LRT *P*-value	Positive sites
Branch model						
A. americanus	M0	−64946.8069	$\omega = 0.03373$	M0 vs. two-ratios model	0.000000013	
	two-ratios model	−64930.6151	$\omega 0 = 0.03518, \omega 1 = 0.01848$			
Bufotes pewzowi	M0	−64946.8069	$\omega = 0.03373$	M0 vs. two-ratios model	0.531545543	
	two-ratios model	−64946.6112	$\omega 0 = 0.03390, \omega 1 = 0.03171$			
Site model						
	M0	−64946.8069	$\omega 0 = 0.03373$			
	M3	−63668.4498	$\omega 0 = 0.00589, \omega 1 = 0.1674, \omega 2 = 112.9303$ p0=0.8121, p1=0.1879, p2=0.00000	M0 vs. M3	0.000000000	[] Not Allowed
	M1a	−64433.7560	$\omega 0 = 0.02376, \omega 1 = 1.00000$ p0=0.9531, p1=0.04689			
	M2a	−64433.7561	$\omega 0 = 0.02376, \omega 1 = 1.0000, \omega 2 = 52.2715$ p0=0.9531, p1=0.04689, p2=0.0000	M1a vs. M2a	0.999941002	[] Not Allowed
	M7	−63763.2701	$p = 0.1689, q = 2.4119$			3584 I 0.654, 3585 T 0.655, 3590 G 0.925, 3594 D 0.942
	M8	−63730.7785	$\omega 0 = 1.00000, q = 2.5907$ p0=0.9894, p1=0.01056, p2=0.1586	M7 vs.M8	0.000000000	Not Allowed
	M8a	−63633.2296	$\omega 0 = 1.00000, q = 3.8578$ p0=0.9986, p1=0.00145, p2=0.1656	M8a vs.M8	0.000000000	Not Allowed

at this site. Amino acid positions 115 and 119 (Fig. S4) are in a part of the ND6 protein that protrudes outside the mitochondrial inner membrane into the intermembrane space (as determined using the TMHMM Server v. 2.0; http://www.cbs.dtu.dk/services/TMHMM/) (*Möller, Croning & Apweiler, 2001*). In this study, *A. americanus* was obtained from the highest latitude and contained both of the two positive selection sites. At 115 and 119 positions of ND6 protein, aspartic acid has a negatively charged polar side chain, whereas glycine has an uncharged side chain with no polar group (*Shiraishi & Kuwabara, 1970*). The amino acid changes in the ND6 protein may have a role in modulating Complex I redox potential and ROS production (*Zhuang & Cheng, 2010*).

Consequently, the above evidence possibly implies that the mitogenomes of these northern species are under natural selection. The changes in the relative mass and electrical charges of amino acids that they encode may be related to adaptive evolution to low temperature environments in *A. americanus*. As the first enzyme complex of the respiratory chain, mitochondrial complex I consists of 45 subunits, its seven hydrophobic subunits being encoded by the mitogenome (*ND1-6* and *4L*) (*Formosa et al., 2018*; *Zhou et al., 2014*). Thus, the adaptive changes in several *ND4* and *ND6* gene sites may affect the proton-pumping process and metabolic performance (*Yu et al., 2011*). *Sun et al. (2018a)* found positive selection on *ND4* from *Tetranychus truncatus* during adaptation to low temperature. *Zhuang & Cheng (2010)* proposed that the modification of *ND6* gene probably improved complex I subunit interactions at low temperatures after analyzing positive selection results. *Lamb et al. (2018)* also found positive selection of the *ND6* gene when tested for evolution caused by climate-linked selection. Furthermore, residue aspartic acid (D, 119) can also be found in the same position in the ND6 proteins of other anurans, such as in the family Ranidae (*Rana dybowskii*, *R. cf. chensinensis* and *R. huanrenensis*), Leptodactylidae (*Leptodactylus melanonotus*) and Microhylidae (*Phrynomantis microps*). We observe that the three frogs in the family Ranidae are mainly distributed in northern China (*Li, Lei & Fu, 2014*; *Dong, Zhou & Yang, 2015*), where temperatures are relatively low. *L. melanonotus* and *P. microps* are distributed near the equator, where temperatures are relatively high. More research is needed to reach definitive conclusions about low or high temperature positive selections in mitochondrial genes (e.g., *Banguera-Hinestroza et al., 2018*; *Ben Slimen et al., 2018*; *Sun et al., 2018b*; *Zhou et al., 2014*). According to this evidence, we can hypothesize that residue aspartic acid (D, 119) in the ND6 protein of *A. americanus* may be related to temperature adjustment and in different anurans may be under different climate-linked selection. However, we did not find evidence for positive selection in the mitogenome of *Bufotes pewzowi* and this suggests that gene adaptations that improve osmoregulation (if they occur) may be associated with nuclear genes. Hence, more information on the evolution of nuclear genomes in toads is needed to analyze the potential adaptation to salinity.

CONCLUSIONS

The complete mitochondrial genomes of *A. americanus* and *Bufotes pewzowi* were successfully sequenced and annotated. Both show the same gene orders and orientation

as occurs in other mitogenomes of Bufonidae, whereas the A+T content of the whole mitogenome in *A. americanus* is the highest among the known species of Bufonidae. It is noteworthy that the *ND1* gene begins with TTG as the start codon and the *trnC* and *trnS* (AGY) genes could not fold into the typical cloverleaf secondary structure in these two toad species, which is a common phenomenon in Bufonidae. Both BI and ML analyses indicated Bufonidae and *Bufo* as monophyletic groups in this study.

Furthermore, foreground branches (*A. americanus* and *Bufotes pewzowi*) are subject to negative selection (ω <1). In the site model, two positive selection sites with BEB values >0.90 were found and both were located in the *ND6* gene. The residue G (115) in ND6 protein can be found in toad species living in northern regions, but residue D (119) in ND6 protein can only be found in *A. americanus*. No positive selection site was found in *Bufotes pewzowi*. The results show that adaptation to low temperature in *A. americanus* may be partly related to evolutionary changes in the *ND6* gene and the residue D (119) in ND6 protein may be linked to temperature adjustment. However, adaptation to high salinity by *Bufotes pewzowi* could not be linked to a modification of its mitogenome.

ACKNOWLEDGEMENTS

ADDITIONAL INFORMATION AND DECLARATIONS

Funding

Grant Disclosures

Competing Interests

Jia-Yong Zhang is an Academic Editor for PeerJ. Kenneth B. Storey is an Academic Editor for PeerJ.

Author Contributions

- Yu-Ting Cai performed the experiments, analyzed the data, prepared figures and/or tables, authored or reviewed drafts of the paper, and approved the final draft.
- Qin Li performed the experiments, analyzed the data, authored or reviewed drafts of the paper, and approved the final draft.
- Jia-Yong Zhang and Dan-Na Yu conceived and designed the experiments, analyzed the data, prepared figures and/or tables, authored or reviewed drafts of the paper, and approved the final draft.

- Kenneth B. Storey analyzed the data, authored or reviewed drafts of the paper, and approved the final draft.

Animal Ethics

The following information was supplied relating to ethical approvals (i.e., approving body and any reference numbers):

The experimental design was specifically approved by the Animal Research Ethics Committee of Zhejiang Normal University.

Field Study Permissions

The following information was supplied relating to field study approvals (i.e., approving body and any reference numbers):

Ontario Ministry of Natural Resources, Wildlife Scientific Collector's Authorization, #1082196, was issued February 1, 2016, expiry date December 31, 2016, to Dr. Kenneth Storey, Department of Biology, Carleton University.

DNA Deposition

The following information was supplied regarding the deposition of DNA sequences:

The complete mitochondrial genome sequences are available at GenBank: MK855099 and MK855100.

Data Availability

The following information was supplied regarding data availability:

The raw measurements are available in the Supplementary Files.

Supplemental Information

Supplemental information for this article can be found online at http://dx.doi.org/10.7717/peerj.8901#supplemental-information.

REFERENCES

Banguera-Hinestroza E, Sawall Y, Al-Sofyani A, Mardulyn P, Fuertes-Aguilar J, Cárdenas-Henao H, Jimenez-Infante F, Voolstra CR, Flot JF. 2018. mtDNA recombination indicative of hybridization suggests a role of the mitogenome in the adaptation of reef building corals to extreme environments. *bioRxiv* 462069 DOI 10.1101/462069.

Ben Slimen H, Awadi A, Tolesa ZG, Knauer F, Alves PC, Makni M, Suchentrunk F. 2018. Positive selection on the mitochondrial ATP synthase 6 and the NADH dehydrogenase 2 genes across 22 hare species (genus Lepus). *Journal of Zoological Systematics and Evolutionary Research* **56(3)**:428–443 DOI 10.1111/jzs.12204.

Bergstrom TM. 2010. A natural history study of Bufo a. americanus, the Eastern American toad, and the phenology of spring breeders in Southwest West Virginia. Master's thesis, Marshall University, Huntington, WV, USA. *Available at https://mds.marshall.edu/etd/403*.

Brandvain Y, Pauly GB, May MR, Turelli M. 2014. Explaining Darwin's corollary to Haldane's rule: the role of mitonuclear Interactions in asymmetric postzygotic isolation among toads. *Genetics* **197(2)**:743–747 DOI 10.1534/genetics.113.161133.

Burland TG. 2000. DNASTAR's Lasergene Sequence Analysis Software. *Methods in Molecular Biology* **132**:71–91 DOI 10.1385/1-59259-192-2:71.

Caballero S, Duchêne S, Garavito MF, Slikas B, Baker CS. 2015. Initial evidence for adaptive selection on the NADH subunit in two of freshwater dolphins by analyses of mitochondrial genomes. *PLOS ONE* **10(5)**:e0123543 DOI 10.1371/journal.pone.0123543.

Cai YY, Shen SQ, Lu LX, Storey KB, Yu DN, Zhang JY. 2019. The complete mitochondrial genome of *Pyxicephalus adspersus*: high gene rearrangement and phylogenetics of one of the world's largest frogs. *PeerJ* **7**:e7532 DOI 10.7717/peerj.7532.

Cao SY, Wu XB, Yan P, Hu YL, Su X, Jiang ZG. 2006. Complete nucleotide sequences and gene organization of mitochondrial genome of *Bufo gargarizans*. *Mitochondrion* **6(4)**:186–193 DOI 10.1016/j.mito.2006.07.003.

Carapelli A, Fanciulli PP, Frati F, Leo C. 2019. Mitogenomic data to study the taxonomy of Antarctic springtail species (Hexapoda: Collembola) and their adaptation to extreme environments. *Polar Biology* **42(4)**:715–732 DOI 10.1007/s00300-019-02466-8.

Castresana J. 2000. Selection of conserved blocks from multiple alignments for their use in phylogenetic analysis. *Molecular Biology and Evolution* **17(4)**:540–552 DOI 10.1093/oxfordjournals.molbev.a026334.

Cheng JX, Cai YT, Zheng YJ, Zhang JY, Storey KB, Bao YX, Yu DN. 2018. The complete mitochondrial genome of *Fejervarya kawamurai* (Anura: Dicroglossidae) and its phylogeny. *Mitochondrial DNA Part B* **3(2)**:551–553 DOI 10.1080/23802359.2018.1467219.

Conant GC, Wolfe KH. 2008. GenomeVx: simple web-based creation of editable circular chromosome maps. *Bioinformatics* **24(6)**:661–862 DOI 10.1093/bioinformatics/btm598.

Dong B, Yang B. 2016. The complete mitochondrial genome of the *Bufo stejnegeri* (Anura: Bufonidae). *Mitochondrial DNA* **27(4)**:2885–2886 DOI 10.3109/19401736.2015.1060421.

Dong BJ, Zhou Y, Yang BT. 2015. The complete mitochondrial genome of the *Rana huanrensis* (Anura: Ranidae). *Mitochondrial DNA Part A* **27(6)**:4551–4552 DOI 10.3109/19401736.2015.1101558.

Fonseca MM, Froufe E, Harris DJ. 2006. Mitochondrial gene rearrangements and partial genome duplications detected by multigene asymmetric compositional bias analysis. *Journal of Molecular Evolution* **63(5)**:641–661 DOI 10.1007/s00239-005-0242-9.

Formosa LE, Dibley MG, Stroud DA, Ryan MT. 2018. Building a complex complex: Assembly of mitochondrial respiratory chain complex I. *Seminars in Cell & Developmental Biology* **76**:154–162 DOI 10.1016/j.semcdb.2017.08.011.

Frost DR. 2014. Amphibian species of the world: an online reference. Version 6.0. NewYork: American Museum of Natural History. *Available at http://research.amnh. org/herpetology/amphibia/index.html*.

Frost DR, Grant T, Faivovich J, Bain RH, Haas A, Haddad CFB, Sá ROD, Channing A, Wilkinson M, Donnellan SC, Raxworthy CJ, Campbell JA, Blotto BL, Moler P, Drewes RC, Nussbaum RA, Lynch JD, Green DM, Wheeler WC. 2006. The amphibian tree of life. *Bulletin of the American Museum of Natural History* **297**:1–291 DOI 10.1206/0003-0090(2006)297[0001:tatol]2.0.co;2.

Gao FL, Chen C, Arab DA, Du Z, He Y, Ho SYW. 2019. EasyCodeML: A visual tool for analysis of selection using CodeML. *Ecology and Evolution* **9(7)**:3891–3898 DOI 10.1002/ece3.5015.

Gao XY, Cai YY, Yu DN, Storey KB, Zhang JY. 2018. Characteristics of the complete mitochondrial genome of *Suhpalacsa longialata* (Neuroptera, Ascalaphidae) and its phylogenetic implications. *PeerJ* **6**:e5914 DOI 10.7717/peerj.5914.

Graybeal A. 1997. Phylogenetic relationships of bufonid frogs and tests of alternate macroevolutionary hypotheses characterizing their radiation. *Zoological Journal of the Linnean Society* **119(3)**:297–338 DOI 10.1111/j.1096-3642.1997.tb00139.x.

Haislip NA, Gray MJ, Hoverman JT, Miller DL. 2011. Development and disease: how susceptibility to an emerging pathogen changes through anuran development. *PLOS ONE* **6(7)**:e22307 DOI 10.1371/journal.pone.0022307.

Hao S, Ping J, Zhang Y. 2016. Complete mitochondrial genome of *Gekko chinensis* (Squamata, Gekkonidae). *Mitochondrial DNA* **27(6)**:4226–4227 DOI 10.3109/19401736.2015.1022751.

Hixson JE, Brown WM. 1986. A comparison of the small ribosomal RNA genes from the mitochondrial DNA of the great apes and humans: sequence, structure, evolution, and phylogenetic implications. *Molecular Biology and Evolution* **3(1)**:1–18 DOI 10.1093/oxfordjournals.molbev.a040379.

Huelsenbeck JP, Ronquist FR. 2001. MRBAYES: Bayesian inference of phylogeny. *Bioinformatics* **17(8)**:754–755 DOI 10.1093/bioinformatics/17.8.754.

Igawa T, Kurabayashi A, Usuki C, Fujii T, Sumida M. 2008. Complete mitochondrial genomes of three neobatrachian anurans: a case study of divergence time estimation using different data and calibration settings. *Gene* **407(1-2)**:116–129 DOI 10.1016/j.gene.2007.10.001.

Jacob Machado D, Janies D, Brouwer C, Grant T. 2018. A new strategy to infer circularity applied to four new complete frog mitogenomes. *Ecology and Evolution* **8(8)**:4011–4018 DOI 10.1002/ece3.3918.

Jiang LC, Liu YB, Zhao L, Ruan QP. 2017b. Complete mitochondrial genome sequence of the Asiatic toad *Bufo gargarizans* (Amphibia, Anura, Bufonidae). *Mitochondrial DNA Part B* **2(2)**:836–638 DOI 10.1080/23802359.2017.1407700.

Jiang LC, Zhang M, Liu J, Ma L, Yu P, Ruan QP. 2018. Characterization of the complete mitochondrial genome sequence of the Asiatic toad *Bufo gargarizans* (Amphibia, Anura, Bufonidae) with phylogenetic analysis. *Conservation Genetics Resources* **10(2)**:173–177 DOI 10.1007/s12686-017-0792-3.

Jiang L, Zhao L, Cheng D, Zhu L, Zhang M, Ruan Q, Chen W. 2017a. The complete mitochondrial genome sequence of the Sichuan digging frog, *Kaloula rugifera* (Anura: Microhylidae) and its phylogenetic implications. *Gene* **626**:367–375 DOI 10.1016/j.gene.2017.05.039.

Kakehashi R, Kurabayashi A, Oumi S, Katsuren S, Hoso M, Sumida M. 2013. Mitochondrial genomes of Japanese *Babina* frogs (Ranidae, Anura): unique gene arrangements and the phylogenetic position of genus Babina. *Genes and Genetic Systems* **88**:59–67 DOI 10.1266/ggs.88.59.

Kan XZ, Li XF, Lei ZP, Wang M, Chen L, Gao H, Yang ZY. 2010. Complete mitochondrial genome of Cabot's tragopan, *Tragopan caboti* (Galliformes: Phasianidae). *Genetics and Molecular Research* **9(2)**:1294–1306 DOI 10.4238/vol9-2gmr820.

Katz U, Garcia-Romeu F, Masoni A, Isaia J. 1981. Active transport of urea across the skin of the euryhaline toad, *Bufo viridis. Pflügers Archiv European Journal of Physiology* **390(3)**:299–300 DOI 10.1007/bf00658281.

Lamb AM, Gan HM, Greening C, Joseph L, Lee YP, Moran-Ordonez A, Sunnucks P, Pavlova A. 2018. Climate-driven mitochondrial selection: A test in Australian songbirds. *Molecular Ecology* **27(4)**:898–918 DOI 10.1111/mec.14488.

Lanfear R, Calcott B, Ho SYW, Guindon S. 2012. PartitionFinder: combined selection of partitioning schemes and substitution models for phylogenetic analyses. *Molecular Biology and Evolution* **29(6)**:1695–1701 DOI 10.1093/molbev/mss020.

Li J, Lei GC, Fu CZ. 2014. Complete mitochondrial genomes of two brown frogs, *Rana dybowskii* and *Rana cf. chensinensis* (Anura: Ranidae). *Mitochondrial DNA Part A* **27(1)**:155–156 DOI 10.3109/19401736.2013.878921.

Lin YB, Tao BF, Fang XD, Wang TT, Zhang JY. 2014. The complete mitochondrial genome of *Lithobates catesbeianus* (Anura: Ranidae). *Mitochondrial DNA* **25(6)**:446–447 DOI 10.3109/19401736.2013.814115.

Liu ZQ, Wang YQ, Su B. 2005. The mitochondrial genome organization of the rice frog, *Fejervarya limnocharis* (Amphibia: Anura): a new gene order in the vertebrate mtDNA. *Gene* **346**:145–151 DOI 10.1016/j.gene.2004.10.013.

Lowe T. 1997. tRNAscan-SE: a program for improved detection of transfer RNA genes in genomic sequence. *Nucleic Acids Research* **25(5)**:955–964 DOI 10.1093/nar/25.5.955.

Lyra ML, Sanchez E, Künzel S, Lötters S, Haddad CFB, Vences M. 2017. The mitochondrial genomes of three species of poison frogs (Anura: Dendrobates). *Mitochondrial DNA Part B* **2(2)**:397–399 DOI 10.1080/23802359.2017.1347830.

Machado DJ, Lyra ML, Grant T. 2016. Mitogenome assembly from genomic multiplex libraries: comparison of strategies and novel mitogenomes for five species of frogs. *Molecular Ecology Resources* **16(3)**:686–693 DOI 10.1111/1755-0998.12492.

Malyarchuk B, Derenko M, Berman D, Perkova M, Grzybowski T, Lejrikh A, Bulakhova N. 2010. Phylogeography and molecular adaptation of Siberian salamander *Salamandrella keyserlingii* based on mitochondrial DNA variation. *Molecular Phylogenetics and Evolution* **56(2)**:562–571 DOI 10.1016/j.ympev.2010.04.005.

Masta SE, Sullivan BK, Lamb T, Routman EJ. 2002. Molecular systematics, hybridization, and phylogeography of the *Bufo americanus* complex in Eastern North America. *Molecular Phylogenetics and Evolution* **24(2)**:302–314 DOI 10.1016/s1055-7903(02)00216-6.

Maxson LR. 1984. Molecular probes of phylogeny and biogeography in toads of the widespread genus *Bufo. Molecular Biology and Evolution* **1(4)**:345–356 DOI 10.1093/oxfordjournals.molbev.a040323.

McBride HM, Neuspiel M, Wasiak S. 2006. Mitochondria: more than just a powerhouse. *Current Biology* **16(14)**:R551–R560 DOI 10.1016/j.cub.2006.06.054.

Möller S, Croning MDR, Apweiler R. 2001. Evaluation of methods for the prediction of membrane spanning regions. *Bioinformatics* **17(7)**:646–653 DOI 10.1093/bioinformatics/17.7.646.

Ni NN, Yu DN, Storey KB, Zheng RQ, Zhang JY. 2016. The complete mitochondrial genome of *Lithobates sylvaticus* (Anura: Ranidae). *Mitochondrial DNA Part A* **27(4)**:2460–2461 DOI 10.3109/19401736.2015.1033697.

Ojala D, Montoya J, Attardi G. 1981. tRNA punctuation model of RNA processing in human mitochondria. *Nature* **290(5806)**:470–474 DOI 10.1038/290470a0.

Pauly GB, Hillis DM, Cannatella DC. 2004. The history of a nearctic colonization: molecular phylogenetics and biogeography of the nearctic toads (*Bufo*). *Evolution* **58(11)**:2517–2535 DOI 10.1111/j.0014-3820.2004.tb00881.x.

Pérez-Ben CM, Gómez RO, Báez AM. 2019. A new Pliocene true toad (Anura: Bufonidae): first record of an extinct species from South America. *Journal of Vertebrate Paleontology* **39(1)**:e1576183 DOI 10.1080/02724634.2019.1576183.

Perna NT, Kocher TD. 1995. Patterns of nucleotide composition at fourfold degenerate sites of animal mitochondrial genomes. *Journal of Molecular Evolution* **41**:353–358 DOI 10.1007/bf00186547.

Portik DM, Papenfuss TJ. 2015. Historical biogeography resolves the origins of endemic Arabian toad lineages (Anura: Bufonidae): evidence for ancient vicariance and dispersal events with the Horn of Africa and South Asia. *BMC Evolutionary Biology* **15(1)**152 DOI 10.1186/s12862-015-0417-y.

Pramuk JB. 2006. Phylogeny of South American *Bufo* (Anura: Bufonidae) inferred from combined evidence. *Zoological Journal of the Linnean Society* **146(3)**:407–452 DOI 10.1111/j.1096-3642.2006.00212.x.

Pramuk JB, Robertson T, Sites JW, Noonan BP. 2008. Around the world in 10 million years: biogeography of the nearly cosmopolitan true toads (Anura: Bufonidae). *Global Ecology and Biogeography* **17(1)**:72–83 DOI 10.1111/j.1466-8238.2007.00348.x.

Pyron RA, Wiens JJ. 2011. A large-scale phylogeny of Amphibia including over 2800 species, and a revised classification of extant frogs, salamanders, and caecilians. *Molecular Phylogenetics and Evolution* **61(2)**:543–583 DOI 10.1016/j.ympev.2011.06.012.

Ren ZM, Zhu B, Ma EB, Wen J, Tu TY, Cao Y, Hasegawa M, Zhong Y. 2009. Complete nucleotide sequence and gene arrangement of the mitochondrial genome of the

crab-eating frog *Fejervarya cancrivora* and evolutionary implications. *Gene* **441**(1-2):148–155 DOI 10.1016/j.gene.2008.09.010.

Ron SR, Mueses-Cisneros JJ, Gutierrez-Cardenas PDA, Rojas-Rivera A, Lynch RL, Rocha CFD, Galarza G. 2015. Systematics of the endangered toad genus *Andinophryne* (Anura: Bufonidae): phylogenetic position and synonymy under the genus *Rhaebo*. *Zootaxa* **3947**(**3**):347–366 DOI 10.11646/zootaxa.3947.3.3.

Sahyoun AH, Bernt M, Stadler PF, Tout K. 2014. GC skew and mitochondrial origins of replication. *Mitochondrion* **17**:56–66 DOI 10.1016/j.mito.2014.05.009.

Schwarz G. 1978. Estimating the dimension of a model. *The Annals of Statistics* **6**(**2**):461–464 DOI 10.1214/aos/1176344136.

Shen YY, Liang L, Zhu ZH, Zhou WP, Irwin DM, Zhang YP. 2010. Adaptive evolution of energy metabolism genes and the origin of flight in bats. *Proceedings of the National Academy of Sciences* **107**(**19**):8666–8671 DOI 10.1073/pnas.0912613107.

Shiraishi A, Kuwabara M. 1970. The effects of amino acids on the labellar hair chemosensory cells of the fly. *The Journal of General Physiology* **56**(**6**):768–782 DOI 10.1085/jgp.56.6.768.

Stamatakis A. 2014. RAxML version 8: a tool for phylogenetic analysis and post-analysis of large phylogenies. *Bioinformatics* **30**(**9**):1312–1313 DOI 10.1093/bioinformatics/btu033.

Storey KB, Storey JM. 1986. Freeze tolerance and intolerance as strategies of winter survival in terrestrially-hibernating amphibians. *Comparative Biochemistry and Physiology. A, Comparative Physiology* **83**(**4**):613–617 DOI 10.1016/0300-9629(86)90699-7.

Storey KB, Storey JM. 2017. Molecular physiology of freeze tolerance in vertebrates. *Physiological Reviews* **97**:623–665 DOI 10.1152/physrev.00016.2016.

Sun JT, Jin PY, Hoffmann AA, Duan XZ, Dai J, Hu G, Xue XF, Hong XY. 2018a. Evolutionary divergence of mitochondrial genomes in two *Tetranychus* species distributed across different climates. *Insect Molecular Biology* **27**(**6**):698–709 DOI 10.1111/imb.12501.

Sun SE, Hui M, Wang MX, Sha ZL. 2018b. The complete mitochondrial genome of the alvinocaridid shrimp *Shinkaicaris leurokolos* (Decapoda, Caridea): insight into the mitochondrial genetic basis of deep-sea hydrothermal vent adaptation in the shrimp. *Comparative Biochemistry and Physiology Part D: Genomics and Proteomics* **25**:42–52 DOI 10.1016/j.cbd.2017.11.002.

Tamura K, Peterson D, Peterson N, Stecher G, Nei M, Kumar S. 2011. MEGA5: Molecular evolutionary genetics analysis using Maximum Likelihood, Evolutionary Distance, and Maximum Parsimony Methods. *Molecular Biology and Evolution* **28**(**10**):2731–2739 DOI 10.1093/molbev/msr121.

Thompson JD, Higgins DG, Gibson TJ. 1994. CLUSTAL W: improving the sensitivity of progressive multiple sequence alignment through sequence weighting, position-specific gap penalties and weight matrix choice. *Nucleic Acids Research* **25**(**14**):4876–4882 DOI 10.1093/nar/25.24.4876.

Vallinoto M, Sequeira F, Sodré D, Bernardi JAR, Sampaio I, Schneider H. 2010. Phylogeny and biogeography of the Rhinella marina species complex (Amphibia,

Bufonidae) revisited: implications for Neotropical diversification hypotheses. *Zoologica Scripta* **39(2)**:128–140 DOI 10.1111/j.1463-6409.2009.00415.x.

Van Bocxlaer I, Biju SD, Loader SP, Bossuyt F. 2009. Toad radiation reveals into-India dispersal as a source of endemism in the Western Ghats-Sri Lanka biodiversity hotspot. *BMC Evolutionary Biology* **9**:131 DOI 10.1186/1471-2148-9-131.

Wang XB, Wang Y, Yue BS, Zhang XY, Liu SL. 2013. The complete mitochondrial genome of the *Bufo tibetanus* (Anura: Bufonidae). *Mitochondrial DNA* **24(3)**:186–188 DOI 10.3109/19401736.2012.744978.

Wang Y, Cao JJ, Li WH. 2017. The complete mitochondrial genome of the styloperlid stonefly species *Styloperla spinicercia* Wu (Insecta: Plecoptera) with family-level phylogenetic analyses of the Pteronarcyoidea. *Zootaxa* **4243(1)**:125–138 DOI 10.11646/zootaxa.4243.1.5.

Waterhouse A, Bertoni M, Bienert S, Studer G, Tauriello G, Gumienny R, Heer FT, De Beer TAP, Rempfer C, Bordoli L, Lepore R, Schwede T. 2018. SWISS-MODEL: homology modelling of protein structures and complexes. *Nucleic Acids Research* **46**:W296–W303 DOI 10.1093/nar/gky427.

Whitehead A. 2009. Comparative mitochondrial genomics within and among species of killifish. *BMC Evolutionary Biology* **9(1)**:11 DOI 10.1186/1471-2148-9-11.

Wolstenholme DR. 1992. Animal mitochondrial DNA: structure and evolution. *International Review of Cytology* **114**:173–216 DOI 10.1016/s0074-7696(08)62066-5.

Xia JH, Li HL, Zhang Y, Meng ZN, Lin HR. 2017. Identifying selectively important amino acid positions associated with alternative habitat environments in fish mitochondrial genomes. *Mitochondrial DNA Part A* **29(4)**:511–524 DOI 10.1080/24701394.2017.1315567.

Xia Y, Zheng YC, Miura I, Wong PBY, Murphy RW, Zeng XM. 2014. The evolution of mitochondrial genomes in modern frogs (Neobatrachia): nonadaptive evolution of mitochondrial genome reorganization. *BMC Genomics* **15(1)**:691 DOI 10.1186/1471-2164-15-691.

Yaghobi S, Vaissi S, Khas ZT, Sharifi M. 2018. Effects of increased salinity on growth, development and survival in early life stages of the green toad *Bufotes variabilis* (Anura: Bufonidae). *Asian Herpetological Research* **9(2)**:129–134 DOI 10.16373/j.cnki.ahr.170083.

Yang JD, Liu JB, Xue R, Chen LM. 2016. Characterization of the mitochondrial genome of *Bufo gargarizans* minshanicus (Anura: Bufonidae). *Mitochondrial DNA P* **27(5)**:3327–3328 DOI 10.3109/19401736.2015.1018206.

Yang ZH. 2007. PAML 4: Phylogenetic analysis by Maximum Likelihood. *Molecular Biology and Evolution* **24(8)**:1586–1591 DOI 10.1093/molbev/msm088.

Ye LT, Zhu CC, Yu DN, Zhang YP, Zhang JY. 2016. The complete mitochondrial genome of *Hyla annectans* (Anura: Hylidae). *Mitochondrial DNA Part A* **27(3)**:1593–1594 DOI 10.3109/19401736.2014.958684.

Yu L, Wang XP, Ting N, Zhang YP. 2011. Mitogenomic analysis of Chinese snub-nosed monkeys: evidence of positive selection in NADH dehydrogenase genes in high-altitude adaptation. *Mitochondrion* **11(3)**:497–503 DOI 10.1016/j.mito.2011.01.004.

Yu DN, Zhang JY, Li P, Zheng RQ, Shao C. 2015. Do cryptic species exist in *Hoplobatrachus rugulosus*? An examination using four nuclear genes, the Cytb gene and the complete MT genome. *PLOS ONE* **10(4)**:e0124825 DOI 10.1371/journal.pone.0124825.

Yu DN, Zhang JY, Zheng RQ. 2012. The complete mitochondrial genome of *Babina adenopleura* (Anura: Ranidae). *Mitochondrial DNA* **23(6)**:423–425 DOI 10.3109/19401736.2012.710214.

Yu DN, Zhang JY, Zheng RQ, Shao C. 2012. The complete mitochondrial genome of *Hoplobatrachus rugulosus* (Anura: Dicroglossidae). *Mitochondrial DNA* **23(5)**:336–337 DOI 10.3109/19401736.2012.690748.

Zhang JY, Luu BE, Yu DN, Zhang LP, Al-attar R, Storey KB. 2019. The complete mitochondrial genome of *Dryophytes versicolor*: phylogenetic relationship among Hylidae and mitochondrial protein-coding gene expression in response to freezing and anoxia. *International Journal of Biological Macromolecules* **132**:461–469 DOI 10.1016/j.ijbiomac.2019.03.220.

Zhang JY, Zhang LP, Yu DN, Storey KB, Zheng RQ. 2018. Complete mitochondrial genomes of *Nanorana taihangnica* and *N. yunnanensis* (Anura: Dicroglossidae) with novel gene arrangements and phylogenetic relationship of Dicroglossidae. *BMC Evolutionary Biology* **18(1)**26 DOI 10.1186/s12862-018-1140-2.

Zhang P, Chen YQ, Zhou H, Wang XL, Qu LH. 2003. The complete mitochondrial genome of a relic salamander, *Ranodon sibiricus* (Amphibia: Caudata) and implications for amphibian phylogeny. *Molecular Phylogenetics and Evolution* **28(3)**:620–626 DOI 10.1016/S1055-7903(03)00059-9.

Zhang P, Liang D, Mao RL, Hillis DM, Wake DB, Cannatella DC. 2013. Efficient sequencing of anuran mtDNAs and a mitogenomic exploration of the phylogeny and evolution of frogs. *Molecular Biology and Evolution* **30(8)**:1899–1915 DOI 10.1093/molbev/mst091.

Zhang P, Zhou H, Chen YQ, Liu YF, Qu LH. 2005. Mitogenomic perspectives on the origin and phylogeny of living amphibians. *Systematic Biology* **54(3)**:391–400 DOI 10.1080/10635150590945278.

Zhang WY, Zhang XJ, Guo R, Tang Y, Zhang YM. 2016. The complete mitochondrial genome of *Bufo raddei*. *Mitochondrial DNA* **27(5)**:3659–3660 DOI 10.3109/19401736.2015.1079843.

Zhou T, Shen X, Irwin DM, Shen Y, Zhang Y. 2014. Mitogenomic analyses propose positive selection in mitochondrial genes for high-altitude adaptation in galliform birds. *Mitochondrion* **18**:70–75 DOI 10.1016/j.mito.2014.07.012.

Zhou Y, Zhang JY, Zheng RQ, Yu BG, Yang G. 2009. Complete nucleotide sequence and gene organization of the mitochondrial genome of *Paa spinosa* (Anura: Ranoidea). *Gene* **447(2)**:86–96 DOI 10.1016/j.gene.2009.07.009.

Zhuang X, Cheng CHC. 2010. ND6 gene lost and found: evolution of mitochondrial gene rearrangement in Antarctic notothenioids. *Molecular Biology and Evolution* **27(6)**:1391–1403 DOI 10.1093/molbev/msq026.